ENERGETICS, THERMAL AND STRUCTURAL PROPERTIES OF HAFNIUM CLUSTERS VIA MOLECULAR DYNAMICS SIMULATION

by

NG WEI CHUN

Thesis submitted in fulfillment of the requirements

for the degree of

Master of Science

September 2016

ACKNOWLEDGEMENT

First of all, I wish to express my gratitude to my supervisor, Dr. Yoon Tiem Leong, and my co-supervisor, Dr. Lim Thong Leng, for their professional guidance and suggestions throughout the whole period of my project and thesis writing. Their motivation and valuable ideas, as well as the tireless commitment in this research, are utmost helpful, especially in leading my learning path as a researcher. For their help and concerns in my studies, I am greatly indebted to both of them.

I would like to thank the Ministry of Higher Education for financial support in term of Fundamental Research Grant Scheme (FRGS) (Project number: 203/PFIZIK/6711348) as well as MyMaster scholarship in covering the tuition fees.

For the immediate colleagues from the theoretical and computational group, I would like to thank them for helping me in my research and pleasantly accommodate my presence. We shared many fruitful discussions that involved a lot of general knowledge, essentially a wide coverage on the latest world news that brings insights to each of us. Special thanks to Mr. Min Tjun Kit, my senior who has offered all kinds of operational and technical support in LAMMPS. Next in line are juniors Ms. Soon Yee Yeen and Ms. Ong Yee Pin for their help in organizing various meetings and sharing of paperwork.

I would like to acknowledge the collaborating group from Taiwan National Central University, Prof. Lai San Kiong and his fellow students, especially Peter Yen for their academic support. Their ideas and comments are the most valuable in helping the competing of this thesis.

Last but not least, I am grateful for my family who supports me in all aspects. They understand and respect my decisions during the completion of my project, and thesis. The hard works and sacrifices they have made encourage me even more to succeed both in life and in academic.

TABLE OF CONTENTS

Acknowledgement		ii
Table of Contents		iv
List of Tables		viii
List of Figures		ix
List of Abbreviations		xii
List of Symbols		xiv
Abstrak		xviii
Abstract		xx
CHAPTER 1:	**INTRODUCTION**	**1**
1.1	Computational Simulation of Atomic Cluster	2
1.2	Objectives of Study	4
1.3	Organization of Thesis	5
CHAPTER 2:	**REVIEWS ON RELATED TOPICS**	**7**
2.1	All about Nanoclusters	8

2.2 Melting in Bulk and Cluster 12

2.3 Chemical Similarity and Shape Recognition 22

2.4 Empirical Interatomic Potential 30

2.5 The Method of Basin Hopping 36

CHAPTER 3: METHODOLOGY 41

3.1 PTMBHGA 42

3.2 Molecular Dynamics Simulation of Hafnium Clusters 47

3.2.1 Simulated Annealing Process 47

3.2.2 COMB Potential 52

3.2.3 Cluster Structures Generation 56

3.2.4 Chemical Similarity Comparison 60

3.2.5 Flying Ice Cube Problem 63

3.3 Post-Processing 68

3.3.1 Global Similarity Index 71

CHAPTER 4: DEPENDABILITY OF COMB POTENTIAL 83

4.1 Geometrical Re-Optimization of Hafnium Clusters 83

4.2 Structural Confirmation of Hafnium Clusters 90

CHAPTER 5: SIMULATED ANNEALING OF THE HAFNIUM CLUSTERS 94

5.1 The Melting Point of Hafnium Clusters 94

5.2 Melting Temperature and Cluster Sizes 102

5.3 Similarity Index and Cluster Melting 106

5.3.1 Hf_{30} 107

5.3.2 Hf_{50} 109

5.3.3 Hf_{99} 111

CHAPTER 6: CONCLUSIONS AND FUTURE STUDIES 114

6.1 Conclusions 114

6.2 Future Studies 115

REFERENCES **118**

APPENDIX A Functionality Form of COMB Potential 125

LIST OF TABLES

		Page
Table 2.1	The example parameters of LJ potential for the noble gases.	14
Table 3.1	The potential parameters of Hf for the COMB potential.	53
Table 4.1	Comparing the clusters obtained via COMB potential after 1 K relaxation and those via DFT geometrical re-optimization with B3LYP basis set (the plmp intra-line comparison).	84
Table 4.2	Comparing the structures of clusters obtained via plmp with COMB (left) and those upon DFT geometrical re-optimization (right) side by side. The size of the cluster is labeled just below the respective pairs of clusters in comparison.	88
Table 4.3	The hafnium clusters of size Hf_4 to Hf_8 in stage 2 of the pg3 process line, along with their DFT total energy value in hartree. (*) indicates structures with lowest energy, while (**) indicates similar structures that are also obtained in the plmp process line.	91
Table 5.1	The melting and pre-melting temperatures obtained from three different approaches. The first four columns are obtained from caloric curves and c_v curves	103

LIST OF FIGURES

		Page
Figure 2.1	Schematic diagram used by Ihsan Boustani (1997) to illustrate the growth of boron cluster from the basic unit of hexagonal pyramid B_7. By adding the repetitive geometrical motif, the cluster eventually forms the infinite quasi-planar surfaces or nanotubes.	11
Figure 2.2	Sample of SCOP2 graph viewer result given by Andreeva et al. (2013), showing the Cro types protein sequence and structure.	23
Figure 2.3	Commonly in use interatomic potential in increasing computational cost Ng et al. (2015a).	35
Figure 2.4	A schematic sketch to illustrate the effect of BH transformation to the PES of a one-dimensional example.	37
Figure 2.5	A schematic sketch indicating the strategy to obtain true global minimum by the way of sampling LLS at a coarse level search with BH method without structural optimization (stage 1), and subsequently undergo a refined geometrical re-optimization of these LLS using DFT method (stage 2). The doted profile in stage 1 represent the simplified staircase topology of the PES.	40
Figure 3.1	Flow chart of the general layout of methodology	41
Figure 3.2	Flow chart for the algorithm in the hybrid PTMBHGA + (LAMMPS / G03) package.	45
Figure 3.3	The melting point and pre-melting point of Hf_{50} with various heating rate. The circle region marks the convergence of melting point lower than certain heating rate.	50
Figure 3.4	The plots of temperature, T against the simulation time step, Δt a) without and b) with time averaging in each $300\Delta t$ time interval.	51

Figure 3.5	A schemetic flow chart of the two parallel process lines. The plmp process line in the left and the pg3 process line in the right. Quantum refinement (geometrical re-optimization) steps are carried out with G03 using the same basis sets and settings in both process lines.	57
Figure 3.6	A schemetic flow chart of intra-line comparison within the plmp process line.	62
Figure 3.7	A schemetic flow chart of inter-line comparison between the plmp and pg3 process lines.	63
Figure 3.8	The condition of Hf_{13} cluster during the heating procedure which encountered flying ice cube artifact, generating excessive kinetic energy. a). The cluster begin to spin in a clockwise manner along the red arrows direction shown, at the beginning of heating procedure. b). The Hf_{13} cluster around 1800K~1900K where the whole cluster start to drift across the simulation box, in addition to the rotation motion, while remain closely bonded like an 'ice' body. The dynamic bonding shown in the figure is kept below 3.2Å, slightly longer than the actual bond length in bulk hafnium.	64
Figure 3.9	The condition of Hf_{13} cluster, showing the bond breaking and bond formation at a) ~850 K, b) ~900 K, c) ~1100 K and d) ~2050 K. Along the simulation time, the cluster did not rotate nor drift across the simulation box, each atom vibrate relative to one another, carry the kinetic energy in them.	68
Figure 3.10	The LLS of Hf_7 cluster. a) The ground state structure. b) The second lowest energy isomer. c) A slight modification was made based on the ground state structure where the bipyramid top was moved closer to the pentagonal base. The green cross indicates center of mass.	73
Figure 4.1	Plot of graphs comparing a) the average bond length and b) the global similarity indexd between COMB structures and that after DFT re-optimization.	85
Figure 5.1	a) The caloric curve and b) c_v curve of Hf_{20} obtained via prolonged annealing process (TNA = total number of atoms in the cluster). The green arrow indicates the pre-melting temperature at $T_{pre} = 1400$ K, and the red arrow indicates the melting point at $T_m = 1850$ K.	96

Figure 5.2	a) The caloric curve and b) c_v curve of Hf_{10} obtained via direct heating process. The green arrow indicates the pre-melting temperature at $T_{pre} = 1350$ K, and the red arrow indicates the melting point at $T_m = 2200$ K.	99
Figure 5.3	a) The similarity index ξ_i and b) fluctuation of similarity index S_{ξ_i} of Hf_{13} obtain via a direct heating process. The green arrow indicates the pre-melting temperature at $T_{pre} = 1600$ K, and the red arrow indicates the melting point at $T_m = 2050$ K.	101
Figure 5.4	Plotting together the estimated pre-melting temperature, T_{pre} and the exact melting point, T_m of Hf clusters of various size n for a) prolonged simulated annealing, b) direct heating process, and c) the global similarity index.	104
Figure 5.5	The estimated melting point of the hafnium cluster against the cluster size n, based on three different approaches.	105
Figure 5.6	a) Similarity index ξ_i curve and b) fluctuation of the similarity index S_{ξ_i} of Hf_{30}. The screenshots show the configuration of the cluster Hf_{30} during that particular temperature.	108
Figure 5.7	a) Similarity index ξ_i curve and b) fluctuation of the similarity index S_{ξ_i} of Hf_{50}. The screenshots shows the configurations of the cluster Hf_{50} during that particular temperature.	109
Figure 5.8	The artifact of single atom drifting away observed in the case of a) Hf_{18} and b) Hf_{26}.	111
Figure 5.9	a) Similarity index ξ_i curve and b) fluctuation of the similarity index S_{ξ_i} of Hf_{99}. The screenshots shows the configurations of the cluster Hf_{99} during that particular temperature	112
Figure 5.10	Hf_{99} upon the equilibration at $T = 3000$K.	113

LIST OF ABBREVIATIONS

AIREBO	Adaptive Intermolecular Reactive Empirical Bond Order Potential
BCC	Body-Centered Cubic
BH	Basin Hopping
BOP	Bond Order Potential
B3LYP	Becke Three Parameter Hybrid Functionals with Correlation functional of Lee, Yang, and Parr
CM	Center of Mass
CNT	Carbon Nanotubes
COMB	Charged-Optimized Many-Body Potential
COR	Center of Reference (Generalized Center of Mass)
DFT	Density Functional Theory
eFF	Electron Force Field
FCC	Face-Centered Cubic
GA	Genetic Algorithm
G03	Gaussian 03 Program
LAMMPS	Large-scale Atomic/Molecular Massively Parallel Simulator
.lammpstrj	LAMMPS Output Trajectory File

LanL2DZ	Los Alamos ECP Plus DZ Pseudopotential for Hafnium
LJ	Lennard-Jones Potential
LLS	Low-Lying Structures
.log	LAMMPS Output Log File
MD	Molecular Dynamics
PES	Potential Energy Surface
pg3	PTMBHGA + G03 Hybrid Package
plmp	PTMBHGA + LAMMPS Hybrid Package
PTMBHGA	Parallel Tempering Multi-Canonical Basin Hopping and Genetic Algorithm
Qeq	Charge Equilibration
ReaxFF	Reactive Force Field
REBO	Reactive Empirical Bond Order Potential
SCF	Self-Consistent Field Procedure
SW	Stillinger-Weber
TEA	Tersoff-Erhart-Albe Potential
USR	Ultrafast Shape Recognition
VMD	Visual Molecular Dynamics Software

LIST OF SYMBOLS

C_a	Center of mass of cluster a
c_v	Constant temperature specific heat capacity
D_{ave}^{χ}	Average bond length
d_m^{χ}	Distance between atoms in a cluster χ, by sorting sequence of m
$d_N(A,B)$	Rogan similarity measure for cluster A and B; $D_N(A,B)$ the normalized form
$d_S(A,B)$	Springborg similarity measure for cluster A and B; $D_S(A,B)$ the normalized form
$d_{s,i}$	Distance of atom s from the center of mass of ith cluster
$\tilde{E}(X)$	Transformed energy topology
E_t or E_T	Total energy
F	Force
f_i	Fitness value of candidate cluster i
k_B	Boltzmann constant
$k_{s,i}$	Difference between the distances of atom s from ith cluster and 0th cluster
m_i	Mass of atom i

M_l	Moments of shape descriptors
$M_p(x_1, \dots, x_n)$	Generalized Mean of variables x
n	Cluster size, or number of atoms
P	Pressure
p	Power of generalized mean, a non-zero real number
p_i	Gaussian weight
q_i	Charge of atom i
r	Distance or position
r_b	Dynamic bond length imposed in visualization
S_{AB}	Normalized similarity index, Tanimoto similarity index
S_{qi}	USR similarity index
S_{ξ_i}	Fluctuation of global similarity index ξ_i
T	Temperature
T_c	Critical temperature in a phase diagram
T_m	Melting Temperature
T_m^{bulk}	Bulk melting point
T_{pre}	Pre-melting temperature

V_{AB}	Overlapping volume of structure A and B
$V_{eff}(1, \dots, n)$	Effective interatomic potential for n interacting particles
V_i	Potential energy of the cluster i
V_{ij}	Interaction potential between atom i and j
v_i^g	Volume of an atom i; v_{ij}^g is the intersection volume of the pair of atoms i and j
V_{LJ}	Lennard-Jones potential
V_n	n-body Gupta potential
V_{pair}	Pair-wise potential
w_i	Weightage factor
δ	Lindemann index
Δt	MD simulation timestep
ε	Depth of the potential well
ξ_i	Global similarity index
ρ	Density
$\rho_i^g(\boldsymbol{r_i})$	Spherical Gaussian as a function of vector position $\boldsymbol{r_i}$ of atom i
ρ_χ^g	Gaussian densities
σ	Interatomic separation at equilibrium

σ_i	'Radius' of an atom
$\langle \sigma_i(t) \rangle_{sta}$	Short-time average distance
χ	Structures label, such as $\chi = A$ or B
χ_i	Chemical potential of atom i

CIRI-CIRI BERTENAGA, HABA, DAN STRUKTUR BAGI GUGUSAN HAFNIUM MELALUI SIMULASI DINAMIK MOLEKUL

ABSTRAK

Kelakuan keleburan gugusan hafnium (saiz $2 < n < 99$) dikaji melalui simulasi dinamik molekul (MD). Interaksi antara atom hafnium diperihalkan dengan keupayaan Charged-Optimized Many-Body (COMB). Keupayaan COMB yang sama digunakan bersama dengan algoritma pengoptimuman global yang dikenali PTMBHGA untuk menjanakan struktur input pada keadaan asas untuk proses MD. Struktur keadaan asas yang diandai telah disahkan apabila berbanding dengan rujukan dan pengiraan prinsip pertama. Selanjutnya, mengesahkan pergantungan potensi COMB dalam proses MD. Biasanya, parameter tenaga digunakan untuk menilai sifat-sifat gugusan. Tesis ini telah menggunakan geometri gugusan selain daripada profil kalori untuk mengaji dinamik semasa keleburan gugusan. Untuk mencapai matlamat ini, algoritma indeks keserupaan global telah direka untuk mengukur tahap persamaan antara dua gugusan. Ia diperoleh berasalkan keserupaan kimia bagi molekul dan mematuhi prinsip sifat serupa. Proses pemanasan MD dijalankan sama ada menggunakan pemanasan langsung atau penyepuhlindapan simulasi berpanjangan. Takat lebur dikenalpasti dengan menggunakan lengkungan kalori, keluk isipadu malar muatan haba dan indeks keserupaan global. Takat lebur gugusan hafnium berubah dengan saiz gugusan, n. Di samping itu, peralihan takat lebur berlaku di pelbagai suhu, bermula dengan peringkat pra-lebur pada suhu T_{pre} sampai peringkat terlebur pada suhu T_m yang lebih tinggi. Ketiga-tiga kaedah bersetuju dengan satu sama lain untuk julat suhu lebur untuk gugusan hafnium. Walau bagaimanapun, didapati bahawa

indeks keserupaan global lebih unggul, kerana ia juga dapat mengesan mekanisme lebur gugusan hafnium.

ENERGETICS, THERMAL AND STRUCTURAL PROPERTIES OF HAFNIUM CLUSTERS VIA MOLECULAR DYNAMICS SIMULATION

ABSTRACT

The melting behavior of hafnium clusters (of sizes $2 < n < 99$) are studied via molecular dynamics (MD) simulation. The interaction between the hafnium atoms is described by Charged-Optimized Many-Body (COMB) potential. The same COMB potential is used with a global optimization algorithm called PTMBHGA to generate the input ground state structures for MD processes. These assumed ground state structures are verified as compared to the literature and first-principles calculation, which further confirm the dependability of COMB potential within the MD processes. Conventionally, the energy parameters are used to evaluate the properties of a cluster. This thesis implements the use of geometry of the clusters in additional to the caloric profile to evaluate the dynamics during cluster melting. Global similarity index, a purpose-designed algorithm to quantify the degree of similarity between two clusters is formulated to achieve this objective. It is derived based on the chemical similarity of molecule and fulfil similar property principle. The heating MD process is carried out either using direct heating or prolonged simulated annealing. Melting point is identified by caloric curve, heat capacity curve and global similarity index. The melting point of hafnium cluster changes with the size of the cluster, n. In addition to that, the melting transition happens across a range of temperature, starting with a pre-melting stage at temperature T_{pre} to total melting at a higher temperature T_m. All the three methods agree with each other for the range of melting temperature for hafnium

clusters. However, it is found that global similarity index is much more superior, as it also traces the melting mechanism of hafnium clusters.

CHAPTER 1

INTRODUCTION

We have already entered into an age of uncertainty about Moore's Law.

(The key conclusion of a presentation by some of the leading technologists at the Intel Corporation during a press conference dated 4th May 2011.)

The world has lived through the digital revolution, and it is still progressing rapidly. The shrinking of the silicon microchips is expected to meet its end in these few years. This is one of the major topics of interest discussed during the latest 2015 International Solid-State Circuits Conference (ISSCC 2015) (Antoniadis, 2015). To date, one of the latest models is the 14 nm 6th generation core processor microarchitecture with the codename Skylake by Intel. Beyond the sub-10 nm, Moore's Law poses many challenges to microchip manufacturer, such as a more demanding device geometry design, higher packing density of transistors, and better performance per cost of manufacturing (Kim, 2015). To resolve the 10 nm technological bottleneck in the near future, researchers are hoping for a new material as a replacement for silicon. Schlom et al. (2008) reported the existing problems within the silicon oxides transistors and a possible replacement by a hafnium-based dielectric. Some other possible candidates do exist, such as the rare-earth $LaLuO_3$ which has a higher dielectric constant. However, the high melting temperature of the proposed alternative substances increases the cost of fabricating transistors made of these substances.

The understanding of the properties of hafnium is essential in order to fully utilize this element in microchip manufacturing. In particular, the properties and thermal behavior of nanoscale hafnium allotropes have not been well studied so far. Studying the properties of hafnium at the nanoscale is experimentally challenging. Theoretical modeling and computational simulation hence provide a convenient and viable approach to complement experimental investigation of nanoscale hafnium.

This work studied the element hafnium in the form of nanoclusters with ranges from 2 to 99 atoms. The stable ground state structures of hafnium clusters are sought, and their thermal properties, including their melting behavior, are numerically studied using molecular dynamics (MD) simulation.

1.1 Computational Simulation of Atomic Cluster

The recent progress in nanotechnology has caused a surge in the interest of searching for a new generation of nanomaterials with exotic or desirable functionalities. Some of these newly established materials are nanoclusters and nanoalloys. Nanoclusters are comprised of fixed number of atoms or molecules that are closely bonded to each other by atomic forces. The number of atoms or molecules that makes up a cluster, n, is normally referred as the size of the nanocluster. Nanoalloys are clusters which composed of more than one element. In such form, an element is no longer behaving like an individual atom, molecule or bulk solid. On top of its varying properties, the structural and energetic behavior of the cluster may also change with size n (Taherkhani and Rezania, 2012).

Besides attempts to understand the behavior of the cluster which is dependent on the size n, attention is also focused on addressing the issue of engineering applications in nanotechnology. In fact, the purpose of studying these nanoclusters is to obtain a better theoretical understanding at atomic level, and to better control the production and their application (Baletto and Ferrando, 2005). One trait of nanocluster is that the properties of the cluster vary as n changes. This enables effective tuning of cluster properties by controlling the size, n. In some cases, certain properties of the cluster could be strongly amplified when the size takes on some specific 'magic number'. The size-dependent properties and existence of magic number provide a handy way for nanomaterial design. The second trait of nanocluster is the exhibition of unique properties that do not occur in their elemental form.

Nanoclusters find their applications in catalysis, magnets design and medical uses (Ferrando et al., 2006). The catalytic effect of nanoclusters is strongly related to their geometry, such as the core-shell structures which are commonly found in bimetallic nanoalloy. For example, Son et al. (2004) demonstrated the example of Ni/Pd core-shell nanoparticles in catalyzing the Sonogashira coupling reactions in a more economical way. The magnetic behavior of some bulk metals sometimes displays a useful nature when they are in the form of a cluster. For example, Park and Choen (2001) managed to synthesize a magnetic nanoalloy of cobalt-platinum via experiments. They claimed that these nanoclusters could be used in nanodevice applications. In biomedical applications, Sun et al. (2006) reported a theoretical study of the effects of gold coating on the magnetic and structural properties of iron clusters of various sizes. In particularly gold metal clusters are of interest in the medical field due to their enhanced optical properties and inert nature of chemical reactions (Giasuddin et al. 2012).

Experiments on a free-standing atomic cluster are rarely reported. For that reason, the understanding of various properties of the nanoclusters requires complementary input through computational simulations and theoretical modeling. The validity of computational simulations founded on the theories of condensed matter. MD, for instance, required the microscopic variables of the ensemble to rescale correctly and the interactions between the particles to be appropriately described by an interatomic potential. Computational simulations of condensed matter systems only become an intensive and active field of research in recent years due to improving CPU capability.

The main aim of the studies mentioned above, among others, include understanding and predicting the properties of material systems at the nanoscale. There are also studies aimed to improve the technique of simulation. This thesis is an endeavor to contribute to the research field of computational nanomaterials by targeting a specific system, the hafnium clusters. Specifically, this thesis attempts an unbiased search algorithm that is able to locate the global minimum of a free-standing cluster in a vacuum and performs MD simulations on the cluster systems at elevated temperatures. The detailed dynamics of the system are analyzed by a novel quantifying method that detects the chemical similarity of the candidate structures.

1.2 Objectives of Study

This work predicts the melting point and analyze the melting behavior of a hafnium nanocluster via MD simulations. The interaction is described by an interatomic potential developed recently, the Charged-Optimized Many-Body (COMB) potential. The dependability of COMB potential in generating the ground state

structures and later on in MD simulations is verified by chemical similarity properties of clusters. In this thesis, the detailed melting behavior of a nanocluster can be visualized in a frame by frame video mode by putting together the coordinates of the atoms in each time step. This approach is successfully being represented by a similarity index analysis created in this study for the visualized trajectory of clusters' geometry. Some of the commonly recognized properties of cluster such as the repetitive geometry motif and size-dependent melting point are being considered in this thesis as well. The simulation is capable of yielding quantitative information and providing convenient qualitative visualization of the atomistic behavior of the cluster during heating process and melting transition.

1.3 Organization of Thesis

Chapter 1 briefly laid out the recent progress of microchips architect as well as some background for the computational simulation of nanoclusters. Moreover, the objectives of study are described in this chapter. The thermal characteristics of a nanocluster, especially those relevant to the melting transition, are discussed in Chapter 2. This chapter also introduced the concept of shape recognition, the role of interatomic potential in molecular dynamics simulation and the method of basin-hopping as a global optimization method. Chapter 3 covered the computational methodology used to define the compatibility of COMB potential as well as the MD simulated annealing procedures for hafnium cluster. The dynamics of heating and melting transition of hafnium clusters are simulated by using the LAMMPS package. This chapter also illustrated the steps taken to overcome the problems arose during the simulation. In Chapter 4, the appropriateness of the choice of COMB potential is

discussed by using the obtained ground state hafnium clusters. The results from MD simulations are then discussed in Chapter 5 by using different post-processing approaches. Lastly, the conclusions and suggestions are given in Chapter 6.

CHAPTER 2

REVIEWS ON RELATED TOPICS

Silicon has played an important part in our lives. However, the jamming of a circuit will soon become one of the obstacles to bring the world another steps forward. According to Moore's Law, the observed number of transistors in an integrated circuit doubles every two years. Researchers are looking for a replacement for silicon as a possible way out to overcome the die shrinkage limit of the silicon transistors. Hafnium was expected as one of the possible element that fulfills all the preliminary tests according to Schlom et al. (2008). Different allotropes of hafnium might provide a possible candidate as a replacement for the silicon. To date, the search for silicon substitution relentlessly continues. This thesis was an effort to investigate the properties of one of the possible substitutes, hafnium, in the form of nanoclusters. The result of this study shall contribute a better understanding of hafnium from the atomistic point of view.

In the first two sections in this chapter, some of the past studies on nanoclusters and their thermal properties are discussed in general. Section 2.3 gives a brief introduction of chemical similarity and some of its latest progress. Furthermore, this thesis also proposes a novel method of similarity index which was derived from the shape recognition method of chemical similarity. This tool is used to study the detailed melting mechanism during the phase change in addition to locating the melting point. Furthermore, the interatomic potential, which is an essential aspect in every MD

simulation, is also discussed in the next section. Finally, the last section of this chapter covers the method of Basin Hopping (BH) which was implemented in a global optimization algorithm known as PTMBHGA (were further discussed in Section 3.1) to generate the ground state structures of hafnium clusters.

2.1 All about Nanoclusters

The keyword atomic nanoclusters refer to a group of atoms with the number of atom, n, larger than two but smaller than the bulk sized thermodynamic limit. The main interest of studying nanoclusters was to find the link that relates the properties of material between the molecular and bulk level. Despite much advancement in the research front, there were still limited experimental data available on cluster. Even if there was, most of the studies on atomic nanoclusters were theoretical and simulations. As a matter of fact, using computational simulation to investigate microscopic system at the atomic level was consensually accepted as an efficacious tool, as the numerical modelling used were parameterized based on the experimental data or first-principles calculations. Commonly accepted methods for first-principles calculation are the density functional theory (DFT) and the Hartree-Fock method.

Predicting the correct ground state structure of a cluster was a non-trivial task. From the point of view of computational simulation, the ground state structure obtained had to be in high geometrical resemblance with the predictions by the first-principles calculations (Soulé et al., 2004). The set of parameters in particular interatomic potential that produces the correct structure can later be used to predict some other physical properties of the nanoclusters. This statement applied generally

for all range of empirical interatomic potential and even the high precision quantum mechanical tight binding approaches.

The small value of n in a cluster gave rise to certain unique properties not present in the bulk solid. The unique symmetry arrangement in the cluster directly influenced the way electrons were arranged, specifically the valence electrons. For instance, the electrical conductivity of carbon nanotubes (CNT) can be modulated by varying the structural orientation of the carbon atoms (Ebbesen et al., 1996). In a metallic solid, the electrons were scattered on the surface of the atoms as a sea of electrons. The mobility of electrons on the surface gave rise to the electronic behavior, such as electrical and heat conductivity. However, the electrons in the nanoclusters were arranged into 'shell' and 'core' sites that were induced from the small value of n. Gould et al. (2015) named this as 'onion' like shells of arrangement. The non-uniform distribution of valence electrons in atomic nanoclusters is a phenomenon known as the electronic charge transfer, which in turn gives rise to certain electronic properties that vary independently from their bulk counterpart.

From computational point of view, the limit of the number of atoms, n in a single cluster was limited by the computing power. However, this was not the case in experiment. Martin et al. (1993) have attempted experimentally to determine the relationship between melting temperature of sodium clusters and the size up to $n{\sim}10^4$. In fact, $n{\sim}10^4$ was not large enough to be considered as a bulk, as the melting temperature was still lower than the bulk melting temperature, T_m^{bulk}. Nonetheless, a group of atoms as large as this was difficult to be processed with computational simulation.

The study of clusters through molecular dynamics simulations was mostly focused on thermodynamical investigation (Calvo and Spiegelmann, 1999). The methodology to do this was well established and diverse, but obtaining the lowest energy structures had always been the primary objective.

The most apparent difference between a cluster and a bulk is the relative binding energy of the structures. An atomic cluster has a higher surface-atoms-to-body-atoms ratio as compared to the bulk. Hence, the surface effect in a cluster is relatively stronger. This causes the atoms in a cluster to be less bonded to each other. Often the atoms are arranged in core-shell order, and some are stable with only the shell, without the core atoms. For examples, nanotubes and fullerenes which were discovered as early as in year 1985. Kroto et al. (1985) showed that C_{60}, which has a unique geometry, is more stable than all other allotropes of carbon.

Some chemists would describe the arrangement of electrons into a new set of orbitals. These orbitals are attributed to the entire group of atoms which act as a single entity. The clusters sometime work as a new chemical species referred to as superatoms, such as the case of Al_{13} which acted like a super chlorine discovered by Bergeron et al. (2004). This cluster was known to be a magic cluster, with magic number $n = 13$. Magic clusters are clusters that are chemically more stable than other non-magic clusters.

In order to obtain the resultant orbitals, the construction of a cluster often involves the imposition of a-priori symmetry constraints. On the other hand, physicists rely on unbiased search algorithm to obtain not a single structure but sometimes multiple lowest energy structures. Chuang et al. (2006) reported a few highly symmetry candidates for the case of Al_{13}, and extended the magic number to $n = 7$,

13, 20, and 22. They also showed that the motif of geometry in single elemental clusters always shows a repetitive unit.

Beside Chuang et al. (2006), Kiran et al. (2005) also confirmed the notion of the geometrical motif in clusters. They showed that boron nanotubes were formed with B_{20} as the cradle motif. B_{20} was found to have a double ring structure. They showed a strong connection between the ring and double ring structures for being the 'embryo' of single-walled nanotubes. In fact, pure boron clusters have been studied earlier by Boustani (1997) and Boustani et al. (1999) via a systematic ab-initio method. It was reported that the boron clusters can be constructed with either hexagonal or pentagonal pyramids, as shown in Figure 2.1. The nanotubular and the quasi-planar structures were shown to be relatively stable and acted as basic building motif of larger boron clusters. Another similar evidence was the case of C_{20}, where the repetitive geometry motif was observed in the ring-to-fullerene transition (Taylor et al., 1994).

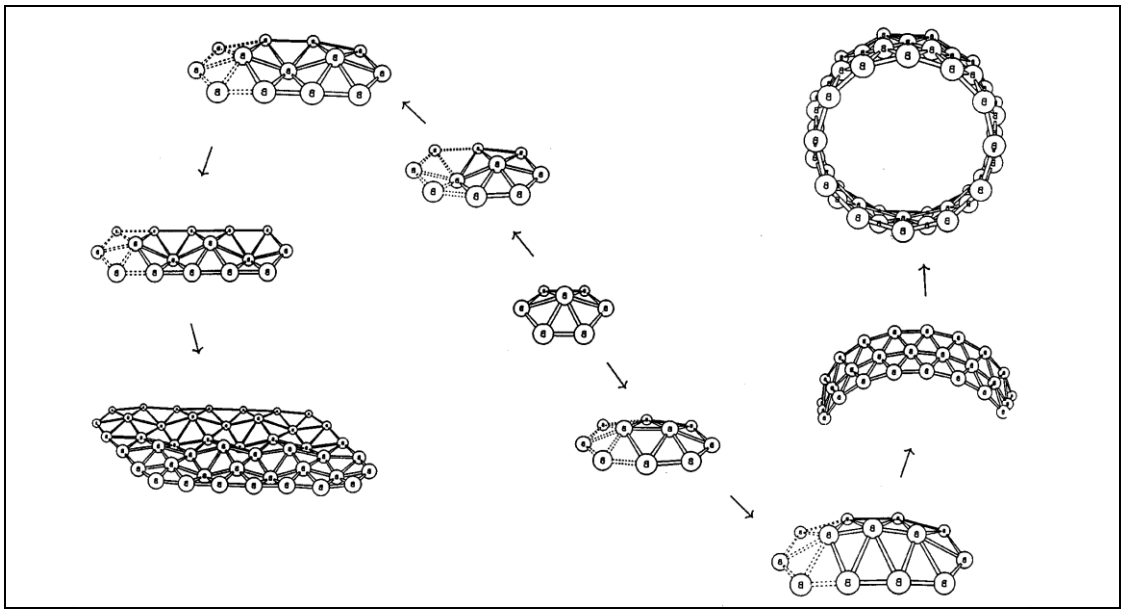

Figure 2.1: Schematic diagram used by Boustani (1997) to illustrate the growth of boron cluster from the basic unit of hexagonal pyramid B_7. By adding the repetitive geometrical motif, the cluster eventually forms the infinite quasi-planar surfaces or nanotubes.

Besides single element nanocluster, dual element cluster was also interested in this field of research. Clusters with multiple elements showed larger varieties of geometrical motifs. Ions in these clusters may arranged themselves into core-shell, pancake (top-bottom or left-right) or even completely randomized arrangements (Rossi et al., 2005). Hsu and Lai (2006) arrived at the same groups of geometries after an extensive search. They included the mixing energy of the clusters to ensure that the potential energy surface (PES) is thoroughly searched for Cu_nAu_{38-n} ($0 \leq n \leq 38$). The magic number also work on bimetallic clusters such as $n = 15$ and $n = 38$. A more recent study by Wu et al. (2011) has laid out the exact combination of atom numbers for Ag-Pd clusters, where the interactions of atoms were modelled with Gupta potential. In that study, Wu et al. prepared two different sets of parameters for the Gupta potential. The first one was fitted using experimental data while the second set was obtained from DFT fitting. They compared the cluster structures for both sets of parameters and found that silver atoms have the tendency to stay at the surface.

2.2 Melting in Bulk and Cluster

The term bulk solid refers to a collection of sufficiently large number of atoms, n. On the other hand, the number of atom of a cluster is less as compared to a bulk. When n grows to a certain large number, transition from a cluster to a bulk will occur. Thus, at this thermodynamic limit of n, the cluster will eventually behave like a bulk solid. Crystals and the amorphous solid are two general types of bulk solid. Bulk metallic solid refers to atoms or ions that occupy the Bravais lattice and possess periodical symmetry of translation in all the axes. For a perfect crystal, all ions have the same arrangement and orientation along every direction. Their arrangements are

classified into distinctive space group. However, in reality, it is implausible to arrange a group of n atoms in such a uniformity over a wide range of displacement. There are always imperfections and dislocations within a crystal. Following that, an amorphous solid does not possess any systematic order in the arrangement of the atoms. The random arrangement of the atoms of an amorphous solid gives rise to a totally different macroscopic behavior as compared to the crystalline solid. Some of the common examples showing such distinctly different behaviors are the existence of high thermal conductivity, electrical conductivity and magnetism in metallic crystals but not in amorphous solid.

Atomic nanoclusters share some characteristics of a bulk solid. On top of this, atomic nanoclusters also resemble the characteristics of a molecule (Menard et al., 2006). Although nanoclusters do not have finite periodicity in the arrangement of atoms, they carry a system of their own symmetry similar to that of the molecular symmetry, which is also known as the point group symmetry. Perfect symmetry only happens to certain magic number clusters. Aside from these magic numbers, some clusters are arranged obviously more random than the others (Ahlrichs and Elliott, 1999). This might result in a behavior integrating both crystalline and the amorphous state.

The crystallization of liquid is a rather complex process, despite the existence of well-tabulated experimental data. Earlier simulations showed that noble gas (e.g. helium gas) forms a face-centered cubic structure with the Lennard-Jones (LJ) potential when the system was cooled. The simulation result agreed with known experimental observation. However, Barron and Domb (1955) predicted the possibility of a different form of liquid crystallization at a lower temperature. This complicates

the crystallization process of liquid. In addition, as for simple pair potential such as the LJ potential, the simulation result would change significantly with any slight modification of the parameters. The functional form of the LJ potential is given in Equation (2.1)

$$V_{LJ}(r) = 4\varepsilon\left[\left(\frac{\sigma}{r}\right)^{12} - \left(\frac{\sigma}{r}\right)^{6}\right] \tag{2.1}$$

where ε represents the depth of the potential well, σ is the interatomic separation at equilibrium and r is the distance between the particles. The fixed parameters here refer to the numerical value of ε and σ uniquely for different element in different chemical environment. Any change to these two parameters will completely alter the potential to model a different element (or no element at all). Table 2.1 presents some examples of parameters for interaction of noble gases (from He to Xe), some as reported by Whalley and Schneider (1955).

Table 2.1: The example parameters of LJ potential for the noble gases.

Interactions pair	ε/k_B (K)	σ (Å)
He-He	10.80	2.57
Ne-Ne	36.38	2.79
Ar-Ar	119.49	3.38
Kr-Kr	166.67	3.60
Xe-Xe	225.30	4.10

The multiple transitions of a crystalline form, or commonly known as allotropy is observed in metal as well. For instance, metal iron (Fe) which is a body-centered cubic (BCC) at room temperature, becomes face-centered cubic (FCC) at 1183 K, but back to BCC at 1667 K and finally melts when it goes beyond 1808 K.

Oxtoby (1990) laid out some of the most common problems in the liquid-solid transition in a bulk crystal. The notion of equilibrium that underlies phase change,

namely the coexistence of phases at critical temperature, T_c is widely accepted. During the latent heat of fusion (melting), the thermodynamic properties are easily documented, but the microscopic changes to the structures between the coexisting phases are not quite understood. There are still some unsolved phenomena such as the local nucleation within a bulk or the dislocation of impurities and surfaces. The dynamical studies of non-equilibrium growth in the microscopic level are very different from the macroscopic observables.

In fact, some of the known premonitory effects close to the melting transition are observed in bulk crystal. For example, substantial changes in volume, compressibility, heat capacity and electric conductivity are observed in bulk crystal long before the bulk melting point T_m^{bulk} (Dash, 2002). These changes are more apparent in clusters, and are known as pre-melting effect. It happens at a temperature T_{pre} before the actual melting point T_m. Breaux et al. (2005) studied the pre-melting effect in aluminium clusters, where the surface melting is observed to occur at a temperature much lower than T_m.

Surface melting occurs as a major event in clusters. In fact, surface melting is an important observation that leads to a complete theory of bulk melting. Faraday (1859) pointed out that the surface melting occurs naturally in any bulk solid. For instance, the melting of water on the surface of ice causes it to be slippery. In fact, this finding can be explained indirectly as the wetting of a solid surface. During this process, any liquid remaining on the solid surface is actually melted from its own surface. There is a model describing the surface energy in term of contact angle (Subedi, 2011). Thus, the macroscopic measurable contact angle becomes a direct measure of the microscopic free energy of the surface liquid layer. Through this

approach, we are able to predict more properties of surface melting and the existence of the metastable state.

Naturally, the interest of study is to find out the asymptotic behavior of atom to bulk. The gradual change of thermal properties with the of size of the clusters, n, is not fully understood. Nevertheless, melting temperature of a cluster being size-dependent is widely accepted, due to most findings supporting the statement (Duan et al., 2007; Liu et al., 2013; Neyts and Bogaerts, 2009; Zhao et al., 2001). However, as reported by Martin et al. (1993), even at $n{\sim}10^4$, the melting temperature of sodium clusters is still lower than the bulk value. It was stated otherwise by Calvo and Spiegelmann (1999) where they suggested the pre-melting, T_{pre} effect to be taken into consideration. From their findings, the melting transition in sodium clusters is said to be at $n > 93$. The core-shell structures of the clusters contribute a significant effect to the surface melting and thus the pre-melting phenomena. Experiments have led to a homogeneous melting model (Effremov et al., 2000) that relates the reduced melting point of a cluster, T_m to that of the bulk, T_m^{bulk} using

$$T_m = T_m^{bulk} - \frac{\alpha}{r} \tag{2.2}$$

where α is a positive quantity with the dimension of [L][θ] which can be determined experimentally, and r is the radius of the particle or cluster. This relationship was derived by Buffat and Borel (1976) from Gibbs-Duhem equation. In the following year, Couchman and Jesser (1977) outlined a direct theoretical study on Sn, In and Au clusters to predict their surface melting. The thermodynamic theory has successfully quantified three features of cluster melting:

1. Melting is initiated at the surface.

2. The existence of an upper and lower limit of the range of melting temperature, T_m.

3. Characteristics of surface nucleation and liquid layer growth are qualitatively captured.

The thermal properties of bulk solid can be obtained through some macroscopically measurable quantities, specifically thermodynamics quantities such as pressure, P, density, ρ, and temperature, T. The thermal properties of a cluster, on the other hand, needs to be obtained by indirect means. Schmidt and Haberland (2002) revised an approach to measure the melting temperature, latent heat, and entropy of some bigger sodium clusters of size ranging from $n = 55$ to $n = 357$, which are derived indirectly from the caloric curve.

Many experimental studies (Schmidt and Haberland, 2002; Martin et al. 1993) have established the following fact regarding the melting of free cluster in comparison to bulk counterpart, namely:

1. The melting temperature, T_m of a cluster is generally lower than the bulk value, T_m^{bulk}.

2. The latent heat of transformation is smaller than the bulk.

3. The melting stage does not occur at a fixed temperature, but begin with pre-melting, T_{pre} over a finite range of temperature.

4. The heat capacity of the finite-sized system can sometimes take a negative value.

In fact, statement one and two are analogous, since the melting temperature, T_m and the latent heat of a cluster show similar fluctuations, while pre-melting is

widely observed though experiments. The first three statements were discussed earlier, but the fourth seems unnatural. A negative heat capacity implies that energy is absorbed with decreasing in the cluster temperature. Heat absorption during melting is commonly understood in terms of latent heat of transformation, where the mean kinetic energy tends to remain constant. In their paper, Schmidt and Haberland (2002) have explained that a finite sized system tends to convert some of the kinetic energy into potential energy in order to avoid partially molten states. Phenomenological observations related to the thermal behavior of cluster will be further discussed in the next chapter from the view point of computational simulation.

In computational simulation, the concept of melting as applicable in the bulk can be similarly applied in microscopic systems. This is a benefit to molecular dynamic simulation whereby the same set of equations of motion is used to solve the interatomic interaction for any kind of system, be it bulk or microscopic.

In a bulk system which is typified by a size of $\sim 10^{23}$ atoms, MD simulation is performed by imposing periodic boundary condition to mimic an extensive body which is formed by a periodic repetition of supercells. However, for finite system such as a cluster, it is possible to simulate the movement of every single atom. The microscopic properties, such as binding energy, temperature, entropy and density of the cluster could be easily computed by sampling the trajectory of every atom for every time step. As far as molecular dynamics are concerned, a free-standing cluster in the vacuum which is practically difficult to set up in experiment can be computationally simulated by choosing a proper empirical interatomic potential. In many occasions, the computational simulation can become relatively cheap to perform. With the ease

of acquiring simulation data, the focus of research effort can hence be devoted to the extraction of physical information from the cluster system.

A cluster behaves differently from both crystals and amorphous solid. The commonly accepted Lindemann criterion of melting is not completely accurate to predict the phase change in cluster. One particular reason for this discrepancy is that the thermal instability of a free-standing cluster creates some errors within the effective range of the interatomic potential in the simulation. This arises due to the existence of multiple basins along the PES. Thus, the initial structure for the simulation has to be ensured such that it lies within the basin of the global minimum (Leary 2000). However, for an expensive interatomic potential, the time required to globally optimize the initial structure is tremendously long and computationally expensive. The numerous approximations and functional form of empirical interatomic potential become a limiting factor as to how accurate a simulation can resemble the real system. This also gives rise to error while solving the equation of motions.

MD simulations allow us to study various characteristics, such as the surface and the core-shells models. Duan et al. (2007) in their molecular simulation of pure Fe cluster showed that for large clusters such as Fe_{300}, the surface can exist as molten phase while the core as solid phase at the same time. The temperature range of melting is, however, narrow and precise. This coexistence of different phases on the surface and in the core proves that the melting of different shells at a different temperature is probable even for pure element clusters. Logically, one would expect that only a core-shell clusters of different elements to undergo this kind of melting pattern. Duan et al. (2007) also made a conclusion that the coexistence is over time for small clusters; whereas the coexistence is over space for big clusters.

When the cluster size is relatively small, the values of melting point, T_m, instead of decreasing with $\sqrt[3]{n}$, could show oscillation. The peaks in the oscillation can be explained by the existence of magic number in finite sized clusters. Such observation was made by Schmidt et al. (1998) in their experiment where the melting point of Na_{147} is higher than Na_{130} by ~ 60 K. The experiment by Schmidt et al. (1998) was considered very sophisticated at that time. It can be said that when the cluster size is very small, the experimental studies become extremely difficult. On the other hand, computational simulation enables easy manipulation of cluster species which will be a complement to the experimental limit.

Another benefit of computational simulation is that the composition and geometrical constraint can be controlled to create a large variety of structures. Kuntová et al. (2008) performed extensive studies on Ag-Ni and Ag-Co bimetallic nanoalloys. They picked only the highly symmetric magic clusters as their candidates, namely $Ag_{72}Ni_{55}$, $Ag_{72}Co_{55}$, $Ag_{32}Ni_{13}$, and $Ag_{32}Co_{13}$. According to the simulation result Ag atoms tend to be sitting in the shell while both the Ni and Co atoms were in the core. Even though the structures of the nanoalloys are similar, the melting behaviors are different. Melting of clusters is greatly affected by the nature of the potential energy surface (PES) that causes a large behavioral change.

The melting data obtained via simulation can be used to study the dynamics of phase change. Comparison between commonly used post-processing methods were discussed by Lu et al. (2009). The most commonly used post-processing method is caloric curves, whereby the binding energy (or binding energy per atom) is plotted against temperature. Another method is the constant temperature specific heat capacity,

c_v, as a function of temperature, which is actually the fluctuations of the caloric curve, given by the equation

$$c_v = \frac{\langle E_t^2 \rangle_T - \langle E_t \rangle_T^2}{2nk_B T^2} \tag{2.3}$$

where E_t is the total energy of cluster, k_B the Boltzmann constant, n the total number of atoms in the cluster and $\langle\ \rangle_T$ represent the thermal average at temperature T. A typical c_v curve appears in the form of a sharp peak at the melting temperature, T_m. Nevertheless, the two methods mentioned above are not the only methods for quantifying the melting behavior of clusters. Some characteristics from simulated annealing process have to be obtained with special treatments. Lu et al. (2009) showed that there is a mismatched in the melting temperature of Co_{13} and Co_{14} clusters, if Lindemann index, δ, was used as a mean to gauge the melting process, as compared to c_v curve. Lindemann index is given by the equations

$$\delta = \frac{1}{n}\sum_i \delta_i \tag{2.4}$$

$$\delta_i = \frac{1}{n-1}\sum_{j \neq i} \frac{\left(\langle r_{ij}^2 \rangle_T - \langle r_{ij} \rangle_T^2\right)^{\frac{1}{2}}}{\langle r_{ij} \rangle_T} \tag{2.5}$$

where r_{ij} is the distance between the ith and jth atoms. Lastly, the dynamics during the cluster melting is studied by short-time averaged distance $\langle \sigma_i(t) \rangle_{sta}$, given by the equation

$$\langle \sigma_i(t) \rangle_{sta} = \sum_j \left| r_i(t) - r_j(t) \right| \tag{2.6}$$

where $r_i(t)$ represents the position of the ith atom at time t, while $\langle\ \rangle_{sta}$ denotes that the average is taken for a short interval of time steps and then plotted against the time. Similar method had been used earlier by Aguado et al. (2001) on Na cluster. Computing the time-average value is troublesome but somewhat could be a solution to the thermal instability in the simulated annealing procedure. The problem of thermal stability is a big obstacle in simulation of cluster melting. Details on molecular dynamics methods used in this thesis were discussed further in Chapter 3.

2.3 Chemical Similarity and Shape Recognition

The method of molecular shape comparison is used in comparing the geometry or spatial configuration of two or more molecular structures to identify the chemical similarity between them (Grant et al., 1996). Molecular shape comparison is an important field of research and application. It is a method with a wide range of applications in the field of informatics, cheminformatics and bioinformatics, such as drug discovery, screening in pharmaceutical studies, nucleic acid sequencing of biological data, protein classifications and identification. The development of structural classification of proteins remain important today, and it is continually improving. Andreeva et al. (2013) recently improved their prototype of structural classification of proteins to the second generation SCOP2 (http://scop2.mrc-lmb.cam.ac.uk/ 1st March 2016). A sample screenshot of using SCOP2 graph viewer is attached in Figure 2.2, showing the classification of Cro regulator proteins based on structural properties and relationships.

The usefulness of molecular shape comparison lies in its ability to transform data into information which in turn leads to a better decision making in drug lead

identification and optimization (Brown, 2005). Shape recognition is by far a method most suitably applied on static molecules. One practical example of dynamical system is the sequential changes of biological molecules across generations. However, it lacks the flexibility to make pattern prediction in dynamical systems which involve constant change in their configuration throughout their historical evolution.

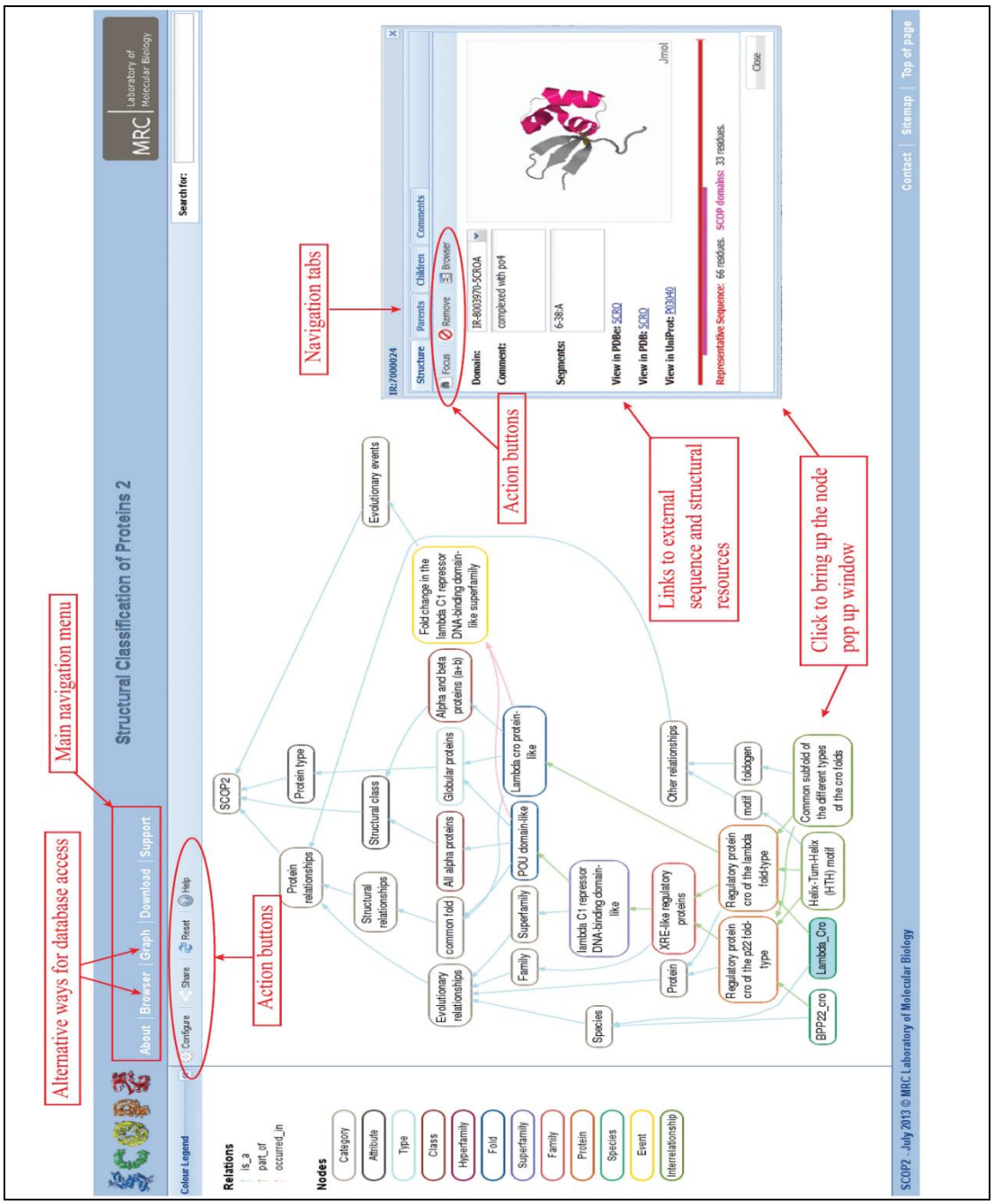

Figure 2.2: Sample of SCOP2 graph viewer result given by Andreeva et al. (2013), showing the Cro types protein sequence and structure.

Virtual screening is a computational procedure to search for chemical similarity to identify and compare the structures of molecules or coupounds from a standard database library, such as the protein data bank. There are different approaches to virtual screening, one of which is similarity-based virtual screening. The formalism of similarity based virtual screening is based on the similar property by Johnson and Maggiora (1990), which stated that the coupounds with higher structural similarity tend to have similar chemical and biological activities. With a suitable approach, one can assign a probability to the activity of the structure under study with reference to the known sample from the database of compounds. However, in the field of informatics, different organizations or companies provide their own unique ways to test for chemical similarity. The degree of similarity between the compared structures predicted by different approach can be differed from one another.

The selected structures for shape identification are normally represented by a binary molecular fingerprint of descriptors, also known as structural keys that containt various visualisable information. For example, the size of the molecule, the number of bonds or type of bondings involved, the active functional groups and the pattern of target structure or substructure (http://www.daylight.com, 1st March 2016). Some descriptors might carry a certain portion of information that outweight others and become less universal for a certain group of compounds. Thus, certain descriptors can work better and faster when the information density is lower, which does not always necessarily so. The descriptors are generally calssified into three types based on the dimensionality of the descriptors. The two-dimensional descriptors such as MACCS, MDL keys, and Daylight are said to perform better than the three-dimensional ones (Oprea, 2002). These two-dimensional descriptors are mostly patented under their own company signature. MDL two dimensional descriptors have been designed to be used